55

STRUCTURAL MAGNETIC RESONANCE IMAGING STUDIES IN SCHIZOPHRENIA

ROBERT W. McCARLEY

> . . . We thus come to the conclusion that, in dementia praecox, partial damage to, or destruction of, cells of the cerebral cortex must probably occur, which may be compensated for in some cases, but which mostly brings in its wake a singular, permanent impairment of the inner life (1).

The window on the brain provided by structural imaging has transformed our view of schizophrenia to one that views the very structure of the brain as altered, a view echoing Kraepelin's prescient statement. Beginning with Johnstone's CT findings of enlarged ventricles (which actually confirmed earlier, less systematic pneumoencephalographic studies), subsequent reports using magnetic resonance imaging (MRI) have provided key information detailing volume reductions in particular brain anatomic regions of interest (ROI). These data have provided the major evidence in support of our current view that schizophrenia is a brain disorder with altered brain structure, and consequently involving more than a simple disturbance in neurotransmission.

Section Organization

The next section is a nontechnical introduction to some of the basic concepts of MRI, and may be read independently of the other sections or skipped by those who wish to concentrate on the clinical data. Subsequent sections discuss the application of structural MRI to questions in schizophrenia research, standards for technical quality and reviews of studies, current MRI findings in schizophrenia (limited to studies with defined ROI), and newer technologies.

THE BASIS OF STRUCTURAL MRI AND PULSE SEQUENCES

Addressing the physics of structural MRI is a major topic on its own, and Brown and Smeleka's book (2) is recommended as a good introduction that demands only a limited background in mathematics and physics. The reader is warned that the following brief exposition is highly (over)-simplified. Essentially, the tissue characteristics sensed by MRI depend on disruptions of a strong external magnetic field. This external field has aligned the orientation of atomic nuclei by aligning the magnetic field of each nucleus that is associated with its spin direction. Because of its biological ubiquity and good magnetic properties, the most commonly used basis element for MRI is hydrogen, which has a single proton in its nucleus. The reader may want to think of hydrogen nuclei as analogous to a large set of spinning tops or gyroscopes. In a state without an external magnetic field, their direction of spin is random, and so is the net magnetization (a vector), because each rotating proton has a magnetic field that is parallel to its axis of rotation. Applying a strong external magnetic field can be thought of as aligning this set of spinning tops in a uniform direction of spin, snapping them to attention, as it were. The resultant population net magnetization can be thought of as vector aligned with the z-axis (vertical axis in our example), perpendicular to the x-y plane, and in the direction of the external magnetic field. The magnetic field strength is described in units of tesla (T) and most current clinical imagers use an external field of 1.5 T.

This vertically aligned population of protons (vertical magnetization vector) is then perturbed by applied radiofrequency (rf) pulses, which can be thought of as having the effect of moving the magnetization vector away from the vertical axis (z-axis); for example, in our analogy, moving the tops from their average vertical orientation to a ''tilt.'' This applied change of the magnetization vector then decays, and, during the course of the decay, give off energy in the form of radiofrequency emissions. It is this emitted energy that provides the key information for MRI scans.

There are two main kinds of information about tissue characteristics derived from this perturbation decay, often referred to as a ''relaxation.'' The T1 relaxation time is the

Robert W. McCarley: Harvard Department of Psychiatry, Brockton VAMC and VA Boston Healthcare System, Brockton, Massachusetts

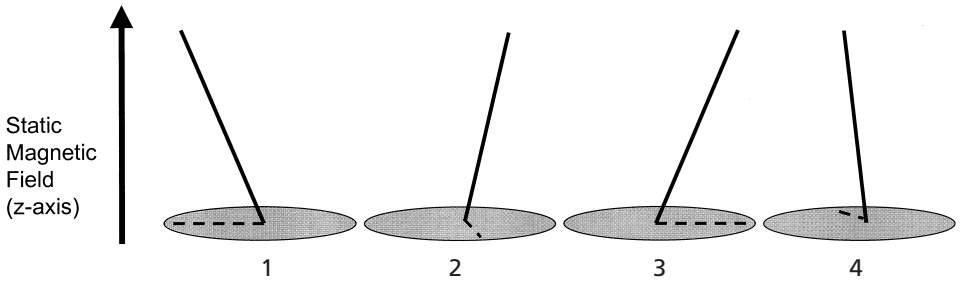

FIGURE 55.1. Illustration of effects of applied magnetic field on hydrogen nuclei (protons, *images 1 to 4*). With only a static magnetic field *(left arrow)* present, all nuclei have the same vertically aligned spin directions parallel to the static magnetic field and the z axis (this state is not illustrated). Application of an rf pulse ''tilts'' the orientation so there is a transverse plane component *(broken line)* in Image 1. Initially all protons precess uniformly, so that images 1, 2, 3, and 4 can be thought of as successive snapshots (successive moments in time) of the counterclockwise precession (rotation) of the net magnetization vector about the z-axis. Over time the protons dephase and show different precession frequencies; as an illustration of this case, images 1 to 4 should be thought of as a single snapshot of individual protons at the same instant in time. There is no net transverse plane magnetic vector because the individual protons show no uniformity of phase.

time constant describing the time course followed by the ''tilted'' magnetization vector in returning to its original orientation. The T1 relaxation time is the time required for this vector to return to 63% of its original vertical orientation value following an rf excitation pulse. Again, in our analogy to spinning tops subjected to a tilt, this T1 is the time required to return to about two-thirds of its original vertical orientation.

The second measure, T2 relaxation time, requires us to think about each nucleus (spinning top) individually. Again and again crudely, one can visualize a group of spinning tops oriented upward (z-axis) and then simultaneously tipped away from this vertical orientation. As everyone who has spun tops or played with a gyroscope knows, if one tilts a top from a vertical orientation, the top will not only tilt but will rotate about the vertical (z-axis), a wobble technically called precessing. Figure 55.1 illustrates this process. In the beginning all the individual tops will wobble (precess) about the z-axis with the same frequency, but gradually they will lose their coherence and wobble at different frequencies, leading to progressively less net magnetization in the x-y plane. T2 is the time required for the coherence to decrease to 37% of its original value. This ''dephasing time'' or T2 relaxation is always less than or equal to T1. Often the term T2* is used to take into account the observed variations in relaxation time owing to inhomogeneities in the tissue being imaged and in the applied magnetic field. The web site, *http://ej.rsna.org/ej3/0095-98.fin/index.htm* has a nice animated illustration of T2 relaxation (on the menu page, select Diffusion and Magnetic Resonance). Of relevance to this description, Pfefferbaum and colleagues (3) found T2 relaxation times were longer in schizophrenic patients than in controls in both gray and white matter, suggesting possible differences in fundamental tissue organization in schizophrenia.

In terms of T1, an rf pulse may ''tilt'' the net magnetization (spin) vector, but usually a second pulse is applied before there is a full return to the vertical orientation, and subsequent rf pulse repetitions lead to a steady-state orientation prior to each new pulse. This new vector depends on a number of values; two are of particular relevance: the T1 relaxation time (how efficiently the protons give up their energy) and number of protons per unit of tissue, *proton density.*

Spatial Localization

The resonance frequency of protons, the frequency at which energy is maximally absorbed by protons, is dependent on the strength of the magnetic field. By applying small magnetic field gradients (typically less than 1% of the total field strength) for short periods of time it is possible to spatially localize the signals resulting from the applied rf pulses. In the presence of a magnetic gradient field each proton will resonate at a unique frequency that depends on its exact position within the gradient field. The MR image is a frequency and phase map of the protons at each point or picture element (pixel) throughout the image. The pixel intensity is proportional to: the number of protons present in the volume represented by the pixel weighted by the T1 and T2 relaxation times. *Different sequences of rf pulses will produce images that mainly reflect one of these variables, and these images are often referred to as proton density-, T1-, or T2-weighted images.* Operationally, the initial step in spatial localization is localization of the rf excitation to a region of space (slice) by the slice selection gradient. When images are viewed, the slice selection direction is always perpendicular to the surface. A second spatial direction is determined by a phase encoding gradient, which differentially alters the precessional frequency of protons at different positions in

the phase encoding direction, thereby enabling spatial localization. In MRI the signal is always detected in the presence of a readout gradient, perpendicular to the slice selection and phase encoding gradient, and producing the third dimension of the image. The readout gradient detects differences arising from both the slice selection gradient and the phase encoding gradient, with the latter varying in amplitude with each repetition of the slice selection and readout gradient.

Pulse Sequences

Appendix A describes commonly used pulse sequences in terms of our knowledge about the relaxation processes for the reader wishing insight into the terminology and rationale of pulse sequences.

STRUCTURAL MRI: WHAT CAN IT TELL US ABOUT SCHIZOPHRENIA?

Structural MRI

In 1984 Smith and co-workers (4) performed the first MRI study of schizophrenia. The capability of structural MRI to provide information about gray and white matter parenchyma of the brain and CSF-filled spaces is new with MRI studies; it represents an important advance over CT studies that poorly visualize parenchyma and can not differentiate gray and white matter. This gray–white differentiation is important for schizophrenia studies, because abnormal tissue classes (tumors, infarcted areas, etc.), which may be detected by CT, have not been found to characterize schizophrenia. The term ''structural MRI'' is used to differentiate it from ''functional MRI,'' where indices of short-duration change (e.g., blood oxygenation) are used; this topic is treated in the second part of this chapter.

Our use of the term schizophrenia is in the sense of a syndrome and not a single disease entity. The current major questions about the schizophrenia syndrome include:

1. What are the brain changes in this disorder? Which areas of the brain are affected?
2. What is the cause of the brain changes?
3. At what life stage do brain abnormalities occur and are they static or progressive? Are they developmental (prenatal and perinatal) and/or progressive?
4. How are brain abnormalities related to clinical symptom abnormalities?
5. Are brain findings in schizophrenia distinct from those in affective psychosis?
6. What are the most effective treatments? Is treatment neuroprotective?
7. Are there structural endophenotypes that will help us in the genetic analysis of the disorder?

Structural MRI studies of schizophrenia have the potential of addressing all of these questions, although space restrictions confine our focus primarily on the first question, which has also been the major focus of empirical studies.

WHAT ARE THE DESIRABLE FEATURES OF A STRUCTURAL MRI STUDY?

We here briefly summarize the features.

1. *Thinner is better.* Smaller units of volume analysis (called voxels, for volume element) allow for more precise determination of the irregular contours of brain regions, by reducing the voxel mixing of the desired region with neighboring structures in the voxel. This mixing is called partial voluming. Many earlier studies used MRI acquisitions with ''gaps'' between slices, with interpolation used to estimate the volume in the ''gap''; this obviously limits precision of measurement. Thus studies with thinner slices (1.5 mm is the current standard), and no gaps between slices, will likely lead to more precise MR morphometric volume measures.

2. *Quantitative versus qualitative analysis.* Early studies relied on subjective, visual ratings of abnormalities. There is now general agreement that computation of volumes of the ROI examined is essential. When raters are used, as is generally the case, inter-rater reliability is important, and should be $r \geq 0.85$. Moreover, the ROI should be objectively and clearly defined, so that others can measure the same entity. Such objectively defined criteria should include detailed specification of the internal landmarks used to define each ROI.

3. *Segmentation.* Segmentation involves sorting the tissue classes into gray matter, white matter, or cerebrospinal fluid (CSF). It seems to us that all studies of cortical gyri should, whenever possible, separate gray and white matter in the analysis, because this is a fundamental distinction in brain tissue; however, not all studies distinguish between gray and white matter, making comparisons with studies that do segment gray and white matter problematic. Finally, segmentation is often automated or semiautomated; unfortunately, there is no agreed-on gold standard for the quality of segmentation, because ''phantoms'' with known composition do not reflect the complexity of the outlines of brain gray or white matter, and postmortem estimates of tissue and fluid volumes may not exactly parallel those *in vivo.* (See ref. 5 for discussion.) Figure 55.2 provides an example of a segmented image with ROI tracing and three-dimensional (3D) reconstruction.

4. *Quality of imager and postacquisition processing.* The quality of the MR scanner is also important and should include technical assessments such as the homogeneity of the magnetic field, which greatly influences the postprocessing segmentation of tissue into different tissue components. Day-to-day assessment of inhomogeneities in the magnetic field is thus a critical quality assurance feature for the quality

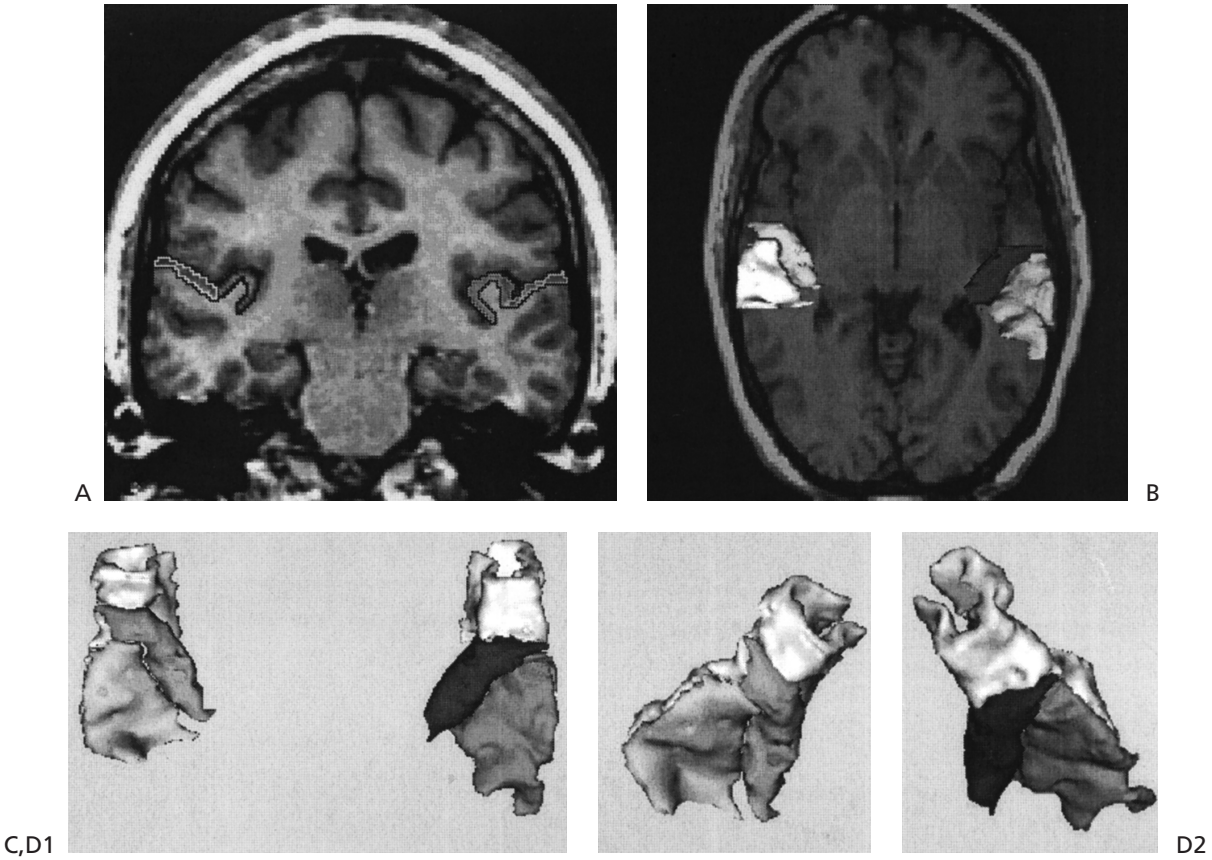

FIGURE 55.2. A: Coronal slice (1.5 mm) through the temporal lobe of a normal control subject. This is a SPGR proton density-weighted image. The regions of interest for the structures are outlined: the gray matter of Heschl's gyrus (HG) is red on subject left and green on subject right. The gray matter of planum temporale (PT) is labeled yellow on subject left and blue on subject right. **B:** Top-down view of the three-dimensional (3D) reconstruction of HG and PT placed atop an axial magnetic resonance slice. This axial slice has been constructed by reformatting the coronal images. Anterior is top. HG is red on subject left and green on subject right, and PT is blue on subject left and yellow on subject right. **C:** 3D reconstruction of the left and right ROI (color-coded as in *B* but from a slightly different angle of rotation than *B*). Note the tubular structure of the gray matter of the STG, most clearly seen anteriorly, where gray codes non-HG, non-PT portions of STG. **D:** 3D reconstructions viewed from a different angle than *C*. (D1 is subject right and D2 is subject left). (Reproduced from Hirayasu Y, McCarley RW, Salisbury DF, et al. Planum temporale and Heschl's gyrus volume reduction in schizophrenia: an MRI study of first-episode patients. *Arch Gen Psychiatry* 2000;57:692–699.)

of the MR scans, and consequently also the quality of the postprocessing of MR images. Most modern imagers have magnetic fields of 1.5 T or greater, which is important for signal-to-noise ratio. Additionally, postacquisition filtering may improve signal-to-noise ratio (6).

5. *Variability and reliability of MRI findings.* An important question is the variability in MRI findings that is to be expected, not only from variation in measurement techniques, but also from physiologic changes. This becomes increasingly important because MR imaging is done at different time points in the disorder. Unfortunately, there are currently very few studies that have examined the extent of changes in MR over multiple measurements, and more careful controlled studies would be useful. Our laboratory found less than 1% variation over gray–white–CSF segmentation values in one subject who had an MR scan on two different days (5). Kikinis and colleagues (7) presented data from a female subject who received 23 MR scans during 1 year. The variance of the intracranial cavity was only 1.2% over the course of the 23 MR scans. Also, there is little evidence of the idea of a physiologic variation in gray or white matter volume throughout the brain in studies with high-resolution MRI techniques. For example, Gur and associates (8) found changes in volume over 2.5 years in whole frontal lobe in schizophrenia without finding changes in volumes of whole-brain and CSF, a finding difficult to reconcile with the idea

of "whole brain variability" in gray or white matter, or CSF caused by hydration or other factors affecting all brain tissue, for example.

HOW SHOULD LITERATURE FINDINGS BE REPORTED IN REVIEWS? EXPERT OPINION VERSUS COUNTING VERSUS METAANALYSIS

The reader trying to shape an informed opinion on the current state of the field (not only structural MRI but any field) relies on reviews with essentially three main approaches, which can be combined.

Expert Opinion

One approach for reviewers is to survey the literature, and then provide an informed opinion as to the summary trends and findings, with specific citations to drive home the points. Many reviews, in fact, adopt this approach of "trust the reviewer." The disadvantage is that the reader cannot form a judgment of the *accuracy of the review's conclusions based on the data presented* without reading the literature.

Counting

This approach tabulates the number of studies with findings supporting or not supporting an abnormality in a particular region. The disadvantage of this approach is that the subject *N* of each study and the effect size are not taken into account.

Metaanalysis

Metaanalysis essentially involves weighting each individual study by a function of its *N* and effect size, and then using this information to produce an estimate of the combined effect size (9–11). *If all studies used equivalent technology and subject populations, this would be the method of choice. However, they do not,* and the reader should realize that: (a) MR scanner technology in the past decade has been changing rapidly; therefore, studies are not quantitatively comparable; (b) the extent of detail varies in anatomically based ROI information used in the measurement of images; (c) there is a wide difference in moderator variables of subject gender, chronicity (age of onset), medication, parental SES, etc.; and (d) metaanalysis, especially of MRI studies, is beset with the difficulty of estimating the number of studies with negative findings that did not get published—Rosenthal's "file drawer" problem (11). Practically, this means one cannot do a review that is both comprehensive and metaanalytically valid, unless the items (a) through (c) had remained constant. Another disadvantage is that many studies must be rejected for reasons of subject or methodologic consistency; this omission has a potential effect of distorting results by omitting technically good studies that could not be included; for example, the metaanalytic study of Nelson and colleagues (12) omitted 45% of the studies on medial temporal lobe found in the literature.

Our summary relies on a combination of these approaches. The conclusions are congruent with our subjective opinions and we provide tabulation of more than a decade's results of MRI studies; however, we are sympathetic to the need to provide more than a simple "box score" of positive and negative results. Accordingly, we have followed a suggestion of Rosenthal (11), and computed the probability of the observed number of positive and negative findings for each region. This is simply done by using a two-tailed alpha level of $p < .05$ for each study finding positive results, and then using the binomial theorem to calculate the overall probability of finding the observed number of positive studies. The resulting overall probability does not assume a normal distribution, but does assume comparability of the studies. (*Caution:* This assumption does not necessarily hold.) Whatever the degree of comparability, this statistic does have the distinct advantage of providing the reader with a sense of the weight of current evidence for each region of interest beyond that of a simple "majority vote," which neglects the odds against an individual study's finding positive results at the $p < .05$ level. We see this as an improvement on simply saying "some studies find . . . but others . . . " and providing the reader a backdrop of estimating the weight of evidence from peer-reviewed studies based on a probability of .05, assuming the prerequisites of metaanalysis hold, and then allowing a subjective "dilution factor" for all of the problems of a metaanalytic analysis.

CURRENT STRUCTURAL FINDINGS IN SCHIZOPHRENIA

A complete review is not appropriate here because the explicit focus of this volume is on summary of main trends and new developments. However, because it seemed essential to us that the reader have at least an overview of structural results in schizophrenia (with references), we have drawn on data from a recent comprehensive review (13). This covered all peer-reviewed schizophrenia studies with control groups during the time period 1987 to May 1998, and to our knowledge is the most recently published comprehensive review.

We summarize here the results from this review, whereas Table 55.1 presents the results and references in tabular form. (Table 2 in the original article summarized the subject *N* and characteristics, and should be consulted for further detail [13].)

Most studies (81% of 31) did not find abnormalities

TABLE 55.1. SUMMARY OF MRI STUDIES REPORTING POSITIVE AND NEGATIVE FINDINGS IN SCHIZOPHRENIA FROM 1987 TO MAY 1998[a] (FROM McCARLEY ET AL., 1999)

Brain Region	% +	% –	Total N	N +	N –	References[b]
Whole brain	19	81	31	6	25	+ [Andreasen 1990,1994b; Gur 1994,1998; Jernigan 1991, Nasrallah 1990] – [Barta 1990; Blackwood 1991; Breier 1992; Buchanan 1993; Colombo 1993; DeLisi 1991; DeLisi 1992; Douphinais 1990; Flaum 1995; Harvey 1993; Hirayasu 1998a; Johnstone 1989; Kawasaki 1993; Kelsoe 1988; Marsh 1994; Nopoulos 1995; Reite 1997; Rossi 1990b,1994b; Shenton 1992; Schlaepfer 1994; Sullivan 1998; Vita 1995; Zipursky 1992,1997]
Lateral ventricles	77	23	43	33	10	+ [Andreasen 1990,1994b; Barr 1997; Becker 1990; Bogerts 1990, Bornstein 1992; Buchsbaum 1997; Corey-Bloom 1995; Dauphinais 1990; Degreef 1990,1992a; DeLisi 1991,1992; Egan 1994, Flaum 1995; Gur 1994; Harvey 1993; Johnstone 1989; Kawasaki 1993; Kelsoe 1988; Lauriello 1997; Lim 1996; Marsh 1994,1997; Nasrallah 1990; Nopoulos 1995; Rossi 1988; Stratta 1989; Suddath 1989,1990; Sullivan 1998; Vita 1995; Zipursky 1992] – [Blackwood 1991; Colombo 1993; Hoff 1992; Jernigan 1991; Rossi 1990b; Rossi 1994b; Schwarz 1992; Schwarzkopf 1990; Shenton 1991,1992]
Third ventricle	67	33	24	16	8	+ [Bornstein 1992; Becker 1996; Dauphinais 1990; Degreef 1990,1992a; Egan 1994; Flaum 1995; Kelsoe 1988; Lim 1996; Marsh 1994,1997; Nasrallah 1990, Rossi 1994b; Schwarzkopf 1990; Woodruff 1997a; Sullivan 1998] – [Andreasen 1990; Barta 1990; Colombo 1993; DeLisi 1991; Schwarzkopf 1992; Shenton 1992; Suddath 1990; Zipursky 1992]
Fourth ventricle	0	100	3	0	3	– [Rossi 1988; Shenton 1992; Stratta 1989]
Temporal lobe (TL)						
Whole TL	62	38	37	23	14	+ [Andreasen 1994b; Barta 1990; Becker 1996; Bogerts 1990; Dauphinais 1990; DeLisi 1991; DiMichele1992; Egan 1994; Gur1998; Harvey 1993; Jernigan 1991; Johnstone 1989; Marsh 1997; Rossi 1988,1989b,1990b,1991; Suddath 1989,1990; Sullivan 1998; Woodruff 1997a; Woods 1996; Zipursky 1992] – [Becker 1990; Bilder 1994asym; Blackwood 1991; Colombo 1993; DeLisi 1992; Flaum 1995; Hoff 1992; Kawasaki 1993; Kelsoe 1988; Nopoulos 1995; Raine 1992; Shenton 1992; Swayze 1992; Vita 1995]
Medial TL	77	23	31	24	7	+ [Barta 1990,1997b; Becker 1990,1996; Blackwood 1991; Bogerts 1990,1993; Breier 1992; Buchanan 1993; Dauphinais 1990; DeLisi 1988; Egan 1994; Flaum 1995; Fukuzako 1996b; Hirayasu 1998a; Jernigan 1991; Kawasaki 1993; Marsh 1994; Ohnuma 1997; Rossi 1994b; Shenton 1992; Suddath 1989,1990; Woodruff 1997a] – [Colombo 1993; Corey-Bloom 1995; DeLisi 1991; Harvey 1993; Swayze 1992; Marsh 1997; Zipursky 1994]
Superior temporal	81	19	16	13	3	
Gyrus						
All studies						
Gray matter	100	0	7	7	0	+ [Hajek 1997; Hirayasu 1998a; Menon 1995; Schlaepfer 1994; Shenton 1992; Sullivan 1998; Zipursky 1994] – None
Gray and white matter (combined)	67	33	9	6	3	+ [Barta 1990; Barta 1997b; Flaum 1995; Marsh 1997; Reite 1997; Tune 1996] – [Kulynych 1996; Vita 1995; Woodruff 1997a]

(continued)

TABLE 55.1. *(continued)*

Brain Region	% +	% –	Total N	N +	N –	References[b]
Planum Temporale	63	37	8	5	3	+ [Barta 1997a; DeLisi 1994; Kwon 1999; Petty 1995; Rossi 1992] – [Kleinschmidt 1994; Kulynych 1995; Rossi 1994a]
Frontal lobe	55	45	33	18	15	+ [Andreasen 1994b; Bilder 1994asym; Breier 1992; Buchanan 1993; Gur 1998; Harvey 1993; Jernigan 1991; Nopoulos 1995; Ohnuma 1997; Raine 1992; Rossi 1988; Schlaepfer 1994; Stratta 1989; Sullivan 1998; Woodruff 1997a; Woods 1996; Zipursky 1992,1994] – [Andreasen 1990; Blackwood 1991; Corey-Bloom 1995; DeLisi 1991; Egan 1994; Kawasaki 1993; Kelsoe 1988; Kikinis 1994; Nasrallah 1990; Rossi 1990b; Shenton 1992; Suddath 1989,1990; Vita 1995; Wible 1995]
Parietal lobe	44	56	9	4	5	+ [Andreasen 1994b; Bilder 1994asym; Schlaepfer 1994; Zipursky 1994] – [Egan 1994; Jernigan 1991; Nopoulos 1995; Sullivan 1998; Zipursky 1992]
Occipital lobe	43	57	7	3	4	+ [Andreasen 1994b; Bilder 1994asym; Zipursky 1992] – [Jernigan 1991; Nopoulos 1995; Schlaepfer 1994; Sullivan 1998]
Localized (L) vs. Diffuse (D) Changes in Cortex	**L %**	**D %**	**Total #**	**#L**	**#D**	
Gray matter	86	14	7	6	1	L [Jernigan 1991; Schlaepfer 1994; Shenton 1992; Suddath 1990; Sullivan 1998; Zipursky 1997] D [Zipursky 1992]
Gray and white matter (combined)	50	50	4	2	2	L [Nopoulos 1995; Bilder 1994asym] D [Andreasen 1994b; Buchanan 1993]
Subcortical Structures	**% +**	**% –**	**Total N**	**N +**	**N –**	
Thalamus	67	33	6	4	2	+ [Andreasen 1990,1994a; Buchsbaum 1996; Flaum 1995] – [Corey-Bloom 1995; Portas 1998]
Corpus callosum	67	33	18	12	6	+ [Casanova 1990; DeLisi 1997; DeQuardo 1996; Gunther 1991; Hoff 1994; Lewine 1990; Raine 1990; Rossi 1988,1989a; Stratta 1989; Woodruff 1993; Uematsu 1988] – [Blackwood 1991; Colombo 1994; Hauser 1989; Kawasaki 1993; Kelsoe 1988; Woodruff 1997b]
Basal ganglia	65	35	17	11	6	+ [Breier 1992; Buchanan 1993; Chakos 1994,1995; Elkashef 1994; Hokama 1995; Jernigan 1991; Keshavan 1995; Mion 1991; Ohnuma 1997; Swayze 1992] – [Blackwood 1991; Corey-Bloom 1995; DeLisi 1991; Flaum 1995; Kelsoe 1988; Rossi 1994b]
Cerebellum	33	66	6	2	4	+ [Andreasen 1994b; Breier 1992] – [Coffman 1989; Flaum 1995; Uematsu 1989; Rossi 1993]
Cavum septi pellucidi	91	9	11	10	1	+ [Degreef 1992b,1992c; DeLisi 1993; Kwon 1998; Jurjus 1993; Nopoulos 1996,1997; Uematsu 1989; Scott 1993; Shioiri 1996] – [Fukuzako 1996a]

Note: asym, finding asymmetry difference only. (Planum Temporale citations are mainly of asymmetry differences and do not use the "asym" qualifier.)
[a]Each study is cited by first author and year.
[b]Full references are listed at the end of this chapter.

of whole brain/intracranial contents, but lateral ventricle enlargement was reported in 77% of 43 studies, third ventricle enlargement in 67% of 24 studies, whereas none of the three studies evaluating the fourth ventricle found abnormalities.

The temporal lobe was the brain parenchymal region with the most consistently documented abnormalities, with 62% of 37 studies finding whole lobe volume decreases. Of all cortical areas surveyed, the superior temporal gyrus most consistently showed volume reduction (81% of 16 studies) and, if the gray matter of this structure was evaluated separately from white matter, all seven studies showed a volume reduction. Fully 77% of the 30 studies of the medial temporal lobe reported abnormalities in one or more of its constituent structures (hippocampus, amygdala, or parahippocampal gyrus). Neuropathologic studies in general support the presence of temporal lobe limbic system abnormalities in schizophrenia (14,15), although some do not (16). Unfortunately, there is a lack of quantitative postmortem studies of temporal lobe neocortex.

Despite the presence of functional abnormalities, frontal lobe structural MRI investigations did not consistently find abnormalities, with 55% of the 33 studies describing volume reduction. In a postmortem quantitative study, Selemon and associates (17) found only a small (8%) reduction in prefrontal cortical thickness, a reduction that was not statistically significant, although noteworthy abnormalities in density of various cell types were present in schizophrenia. This and the MRI findings suggest that frontal lobe volume reductions may be small, and near the threshold for MRI detection. The parietal and occipital lobes have been much less studied, and there are about the same percentage of positive and negative findings in each. Most of the seven studies of cortical gray matter (86%) find that volume reductions are not diffuse, but are more pronounced in certain areas, as might be anticipated from the preceding statistics on individual regions of interest.

About two-thirds of the studies of subcortical structures report positive findings, including the six studies of the thalamus, 18 studies of the corpus callosum, and 17 studies of the basal ganglia. Basal ganglia tended to show increased volume when patients were on typical but not on atypical neuroleptics. The cerebellum had mainly negative findings (in four of the six studies), but was not studied with the same volumetric precision as other ROI. Almost all (91%) of the 11 studies of cavum septi pellucidi (CSP) showed that schizophrenics have less fusion of the septum, a developmental abnormality probably linked to limbic system pathology.

Statistics

The binomial theorem computation (using $p < .05$ for a positive study) shows that *all ROI* surveyed in Table 55.1 show a two-tailed $p < .05$ for the number of positive studies, except for the fourth ventricle and cerebellum ($p = .66$), and all ROI had p's $\leq .002$ except for the occipital lobe (.004). Again, caution should be exercised on the strength of these probability estimates because comparability is not strict and an (unknown) percentage of studies with negative results may not have been published.

Clinical Symptom Implications

Clinical scale data suggest that positive symptoms (and disorganization in a three-factor model) may be most closely related to temporal lobe volumetric abnormalities, whereas more limited evidence supports, in some studies, a relationship between negative symptoms and frontal lobe MRI abnormalities. Finally, there now appears to be growing evidence that MRI abnormalities differ in affective (bipolar) psychosis and schizophrenia, with reductions in neocortical gray matter, especially in temporal and prefrontal neocortex being especially prominent in schizophrenia. (See McCarley and co-workers 1999 for a more complete review and Sheline [this volume] for a review of structural MRI in affective disorder [13].)

The presence of CSP and sulco-gyral abnormalities (for the latter, see Kikinis and colleagues) (18) and abnormalities in first-episode patients all suggest a possible developmental origin. However, there are growing (although still limited) data pointing to progression of volumetric abnormalities over time. This suggests that both developmental and progressive features may be present in schizophrenia; these are consistent with, we hypothesize, a ''two-hit'' model of schizophrenia.

AUTOMATING STRUCTURAL MRI ANALYSIS: BRAIN WARPING AND VOXEL-BASED ANALYSIS

The tedious task of manual definition of regions of interest by tracing outlines—even if assisted by automated segmentation—has prompted interest in using automated methods of MRI analysis. The two (closely related) major classes of methods are: (a) brain warping, using a standard or ''atlas brain'' to compare and define features on subject brains, and (b) voxel-based analyses. Because these techniques, although promising, are new and thus far have limited data on validity, we have not included the studies in the summary table of ROI findings. This section concludes with a brief discussion of shape analysis, often based on the brain warping techniques described in the first part of this section.

Brain Warping

In one use of this technique the ROI definitions and anatomic features of an index template (atlas brain image) are warped (mapped) onto a new case (target image). In this

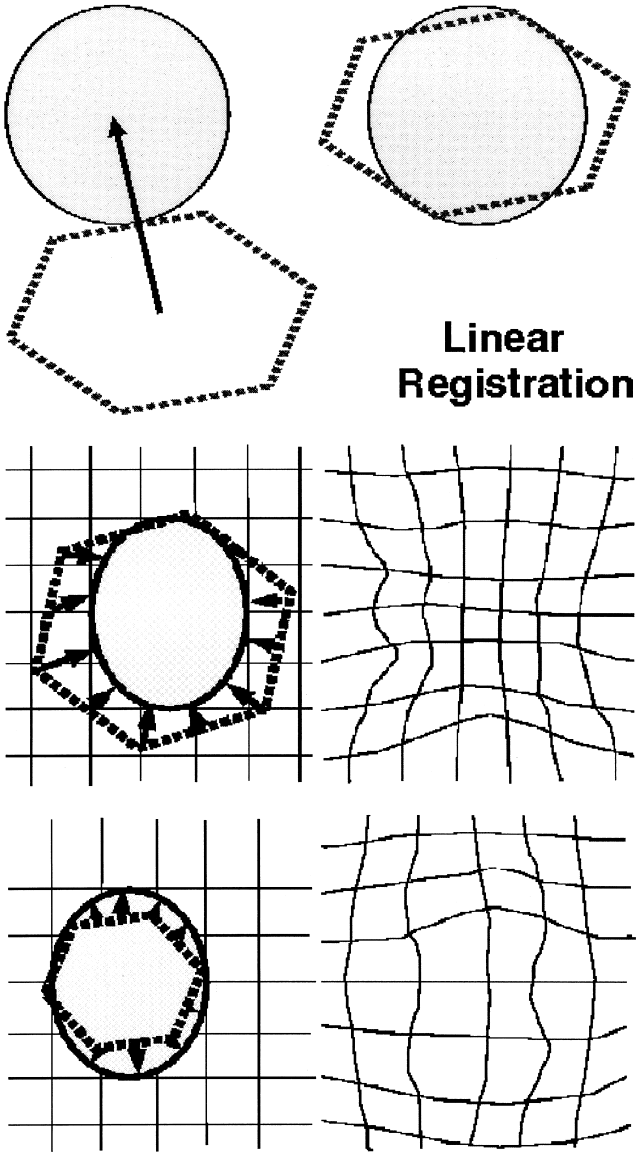

FIGURE 55.3. Schematic of brain image warping. An ''atlas'' image *(red hexagon)* is warped (mapped) onto a new ''patient'' image *(yellow oval)*. **Top:** A simple uniform linear transformation (translation, rotation or scaling) does not work. Instead, nonlinear transformations are used to ''warp'' the ''atlas'' image onto the ''patient'' image *(middle and bottom panels)*. This warping resulted in a ''vector field'' *(blue arrows)*. The nonuniform displacement of each pixel is then represented in the right field of Fig. 55.1, by means of the deformation of the rectangular grid (the elastic membrane). Examples are presented for atlas contraction *(middle panel)* and dilatation *(bottom panel)*.

context, the atlas brain can be compared to a rubber brain, which is stretched and compressed nonlinearly in order to match the contours of the new brain. At the end of the registration, all the structures previously defined for the atlas brain are also defined for the new brain image. In general, the first step in matching the atlas brain and subject (patient or object brain) is *linear registration* to correct for the differences in size, rotation, and translation between the two brain images. This step is illustrated in the first panel of Fig. 55.3. (Parenthetically, linear transforms use scaling, translation and rotation uniformly for each element [voxel], whereas nonlinear transforms use different and more complicated transforms for different voxels.)

Nonlinear Elastic Matching

The atlas information can then be projected into other MRI scans by applying an elastic match (i.e., warping the atlas into the shape of the new brain image). The global registration technique used by our lab (19) to match an anatomic MR atlas with defined ROI onto new-segmented MR images, was based on the theory of elastic membranes (20,21), and was similar to Grenander and Miller's (22) approach. The elastic membrane model can be intuitively understood as the deformations occurring when a set of points on the membrane is stretched. The goal of the elastic matching algorithm was to find a 3D *vector deformation field* that transformed the source data set (atlas) so that it matched the target data set (patient) with the greatest fidelity, that is, maximized the local similarity between the two data sets under the constraint of using a restricted set of ''stretches'' of the membrane. The middle and bottom panels of Fig. 55.3 show, in a cartoon, how contraction and expansion of particular voxels lead to a match between the atlas brain and the target brain. The right-hand part of these panels graphically illustrate the voxel-by-voxel deformation (stretching or compression) resulting from the *vector deformation field* used to transform the atlas image. We note that other choices of an ''index brain'' include the probabilistic atlas used by the Montreal Group (23) and interpolated data from an anatomic atlas, as used by Gee and colleagues (24).

Brain Warping: How Good Is It?

Any new technique must be validated, and brain warping is no exception. The current gold standard is manual ROI definition. The technique used by Iosifescu and co-workers (19 and unpublished data) was compared with manual ROI definition for volumes. Agreement on volumes over 28 subjects (half schizophrenia patients and half controls) was 97% for whole brain volume, 97% for whole white matter, 91% for whole gray matter, 96% for thalamus (both sides), 93% for putamen, 91% for caudate nucleus, and 76% for globus pallidus. A more rigorous and better method of comparison is the extent of overlap of voxels in the manually defined ROI with those in the automated definitions. In measurements of 20 brain cortical and subcortical brain structures on one brain image the extent of voxel-by-voxel correspondence, was defined as:

$$\frac{(\#\text{ voxels in manual ROI also in automated ROI})}{(\#\text{ voxels in manual ROI})}$$

This averaged 90% for subcortical structures and 98% for total gray and white matter volumes; however, for cortical gyri the overlap averaged only 60%. The automated computer algorithm assumed the neuroanatomic variability among subjects to be a topologic invariant. However, cerebral gyri frequently split in two in some subjects, whereas they remain one single structure in others. These differences could not be taken into account by the automated registration in its present form. Taken together, these data suggest:

1. Each automated warping procedure should be compared with the results using manual ROI definitions.
2. Accuracy may be good for subcortical structures (because of their relatively small variability in shape) and total brain gray and white matter.
3. Accuracy is questionable for the neocortex, because of the irregularity of sulco-gyral patterns.

A recent use of the technique of warping is to use the *vector deformation field* to provide a statistical test of whether each voxel is significantly displaced or not (25). (See Fig. 55.3 for a description of extent and direction of warp.) This methodology does not attempt to map gyrally defined ROI, but rather looks at changes in gray matter on a global or regional basis, often using Talairach space.

Gaser and colleagues (26) compared the 3D vector deformation fields required to warp each voxel of an index brain (source not specified, presumably that of the Talairach atlas) onto spatially normalized brains of a large group of schizophrenic patients ($n = 85$) and controls ($n = 75$). They then computed the statistical significance of the difference between the schizophrenic patients' and controls' deformation fields, finding volume reduction bilaterally in Talairach spatial locations corresponding to thalamus and superior temporal gyrus and unilateral reductions in the superior and middle frontal gyrus, precentral gyrus, lingual gyrus, and cerebellum. This study forms a good transition to the next section because the spatial normalization techniques and the nonlinear registration method, those of SPM99 and Ashburner and Friston (27), respectively, are described in the following section.

Voxel-Based Morphometry

Ashburner and Friston (27) define this technique as "a voxel-wise comparison of the local concentration of gray matter between two groups of subjects," and have provided a detailed description of this methodology, closely related to that of SPM99. As a first step, this method takes all subject images and normalizes them to the same stereotaxic space, using procedures similar to those used in SPM for fMRI and PET data. This procedure involves an initial linear (affine) match (similar to that described for brain warping) followed by a nonlinear registration using smooth spatial basis functions. These authors emphasize that this spatial normalization "does not attempt to match every cortical feature exactly, but merely corrects for global brain shape differences," thereby differentiating it from more exact attempts at a match, as discussed in the brain warping section. The second step involves segmentation of the normalized images into gray matter, white matter, and CSF. The third step is smoothing using a convolution with a Gaussian kernel, which leads to each voxel being the mean of gray matter density for it and, to a spatially progressively lesser degree, its neighbors. The last step is statistical analysis using the general linear model to identify regions of gray matter concentration that are significantly related to the variable under study (if normality is not present a nonparametric statistical analysis is used).

Compared with manually drawn ROI, this technique has the following clear advantages: (a) enabling of regional comparisons throughout the whole brain without the restrictions of a few selected areas used in the typical manually drawn region of interest methodology; (b) the reduction of labor; and (c) the ability to use large samples with an attendant increase in statistical power as a corollary to (b).

Unfortunately, however, there as been an absence of work comparing the spatial specificity and sensitivity of voxel-based analysis with manual ROI analysis, the current standard, and thus the question of validity has been incompletely addressed.

Wright and co-workers (28) have undertaken some comparisons with manual ROI. They performed manual area measurements of the head of the caudate in the transverse slice 12 mm superior to the intercommissural plane in the untransformed data. They then compared these with voxel values in the transformed data at coordinates corresponding to the center of the caudate in Talairach space for each of 20 the subjects. They found Pearson product–moment correlations between the area measurement and the voxel gray matter values for the transformed data for the 20 subjects to be about $r = 0.8$. These data do not, unfortunately, provide information on spatial specificity in terms of a measurement of the boundaries of the caudate in the untransformed data for the 20 subjects and the transformed data. Nor do these data, taken from the center point of a regular structure, provide any clear information on how well the transformation would work on the much more irregular cerebral cortex. Because one of the findings with transformed data was decreased gray matter in the schizophrenic group in the voxels corresponding to the right amygdala, one would have liked to see a comparison with manually drawn ROI in this structure as a way of validating the voxel analysis (and/or a comparison in the other regions found to be abnormal, the temporal pole/insula, and left dorsolateral prefrontal cortex). Wright and associates did find that voxel analysis could detect artificial "lesions," created by setting gray matter content to zero in a group of voxels, including a 4- $\times$ 4-mm bar and a 12- $\times$ 25-mm grid. They did not try more realistic "lesions" with parametric variation of degrees of lesser gray matter content; nor did they quantify

the spatial specificity. In concluding the discussion of this technique, Wright and colleagues voiced the important caveats that voxel based morphometry may not detect "very small gray matter reductions, gray matter reduction in areas of high variability in gray matter volume or gray matter reductions with an inconsistent location."

A direct comparison of manual ROI and voxel-based analysis would seem to be a high priority, because some estimate of the specificity and sensitivity of voxel analysis for various brain regions and ROI could be formed. Until such validation procedures are done, any results with voxel-based morphometry (VBM) will, of necessity, be viewed by many workers in the field as tentative. Because of the importance of the validity question, our laboratory has recently begun to compare SPM99 VBM results with traditional ROI analysis (Kubicki and colleagues, unpublished data). For VBM applied to whole brain, only the left posterior superior temporal gyrus region was significantly different between schizophrenic and control groups, a finding consistent with our ROI analysis. In a less statistically less stringent analysis (taking into account peak z values and voxel cluster extent), there was significance bilaterally in the anterior cingulate gyri and insula (regions not examined with ROI), but not in medial temporal lobe where ROI analysis showed differences.

Taken together, these data suggest the following methodologic conclusions:

1. Each VBM study should be compared with manual ROI definitions until validity is established.
2. VBM may be useful for generating hypotheses to be validated with traditional ROI analyses.
3. Much work remains to be done in comparing the validity of VBM and ROI analysis, and formulating reasons for any differences.

Shape Analysis

It is readily apparent that ROI shape as well as volume may carry information about pathology. Casanova and colleagues (29) used 3D Fourier techniques to characterize shape of temporal lobe regions, finding schizophrenics and controls differed. However, Fourier techniques cannot pinpoint where in the shape the abnormality occurs, as can brain warping and other methodologies. Csernansky and associates (30), using a variant (based on Grenander's work) of the brain warping techniques described in the preceding, found that maximal differences between controls and the schizophrenia subjects were localized to the lateral aspect of the head of the hippocampus and medial aspect of the body, where the subiculum is found. The study of shape using a number of different algorithms is a current area of very active interest in MR schizophrenia research, especially in the study of the corpus callosum.

DIFFUSION TENSOR MR IMAGING

This is a new MRI technology that is able to provide information on the orientation and integrity of fiber tracts. In diffusion tensor imaging (DTI), a tensor describing local water diffusion is acquired for each voxel; crudely, this tensor can be thought of as a mathematical description of the direction and velocity component of diffusion relative to the orientation of the chosen coordinate system, or "basis." Diffusion may be "isotropic," equal in all directions, as occurs in CSF, and the diffusion volume (3D representation of diffusion pathways) has a spherical geometry in this case. Or diffusion may be "anisotropic" (e.g., not isotropic) and greater in one direction, in which case there is an ellipsoid shape. The limiting case for maximal anisotropy is an infinitely long and thin cylinder. In white matter fiber tracts diffusion is mainly in the direction of the fibers. Factors that affect the shape of the apparent diffusion tensor (shape of the diffusion ellipsoid) in the white matter include the density of fibers, degree of myelination, average fiber diameter, and directional similarity of the fibers in the voxel. For example, the DTI-measured diffusion coefficients are larger when measured along (parallel to) white matter fibers (in the range of 1.0×10^{-3} mm^2/sec) than across the fibers (in the range of 0.6×10^{-3} mm^2/sec). The geometric nature of the measured diffusion tensor within a voxel is thus a meaningful measure of fiber tract organization.

The degree of anisotropy in schizophrenia has been investigated in two recent studies. Using DTI, Buchsbaum and associates (31) reported evidence of lower diffusion anisotropy in some inferior portions of prefrontal white matter in patients with schizophrenia than in controls. Lim and co-workers (32) found that abnormally low white matter anisotropy in patients with schizophrenia was present in both hemispheres and was widespread, extending from frontal to occipital brain regions. For group statistics, Lim and co-workers used the median value of voxel anisotropy (measured as fractional anisotropy; 1 is maximal and 0 minimal) in each slice within the white matter regions of interest in the control and schizophrenia groups. These studies raised the important question of whether white matter connectivity is disturbed in schizophrenia, although Lim and colleagues caution that the proper statistical measures for DTI are still being worked out.

A recent technical advance in DTI has been line scan diffusion imaging (LSDI). This method, in contrast to the commonly used diffusion-sensitized, ultrafast, echo-planar imaging (EPI) technique, is less sensitive to gross motion and cardiovascular pulsations. LSDI also has higher resolution, exhibits minimal image distortion, and does not require cardiac gating, head restraints, or post-processing image correction. It also can be implemented without specialized hardware on all standard MRI scanners.

Recent work has focused on measurements extending beyond the scalar measurement of the degree of anisotropy

in a voxel to characterizing the spatial trajectory and orientation of fiber tracts. Although the individual axons and the surrounding myelin sheaths cannot be revealed with the limited spatial resolution of *in vivo* imaging, distinct bands of white matter fibers with parallel orientation may be distinguished from others running in different directions if MRI techniques are sensitized to water diffusion and the preferred direction of diffusion is determined. Figure 55.4 shows the degree to which orientation of fiber tracts can be quantified and displayed using color-coding. An important point for summarizing data made by Westin and associates (33) is that remaining within the tensor domain when processing is useful, as contrasted with operating on scalars and vectors to produce summary statistics. In processing DTI images, it is important to note that averaging of a diffusion tensor field and then deriving a scalar measure from the averaged field is not the same as averaging a scalar field derived from the original field. By using geometrically defined diffusion measures on locally averaged tensors local directionality consistency can be determined (e.g., existence of larger fiber tracts). This averaging approach can be used to derive a tensor field that will describe macrostructural features in the tensor diffusion data. For example, a measure of linearity derived from the averaged tensor field can be used for quantitative evaluation of fiber tract organization.

Still another promising application of DTI is tracking white matter tracts. The operation begins with a seed point in a voxel element and then generates a tracking sequence

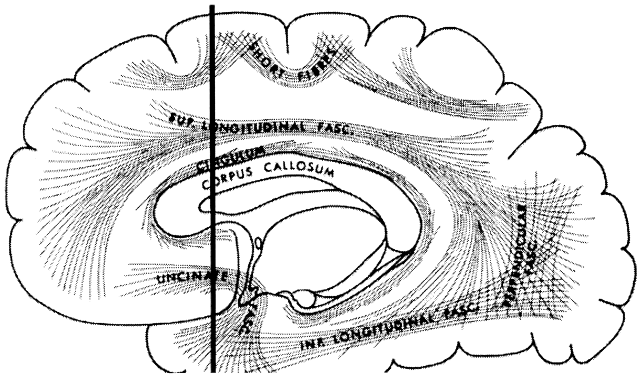

A

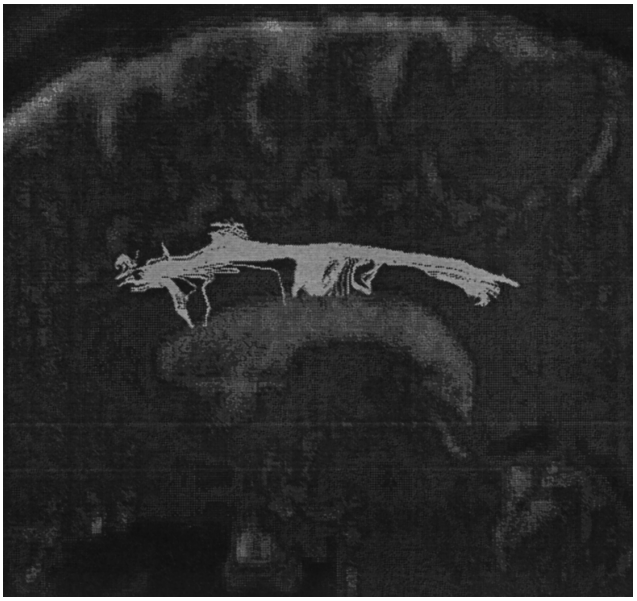

C

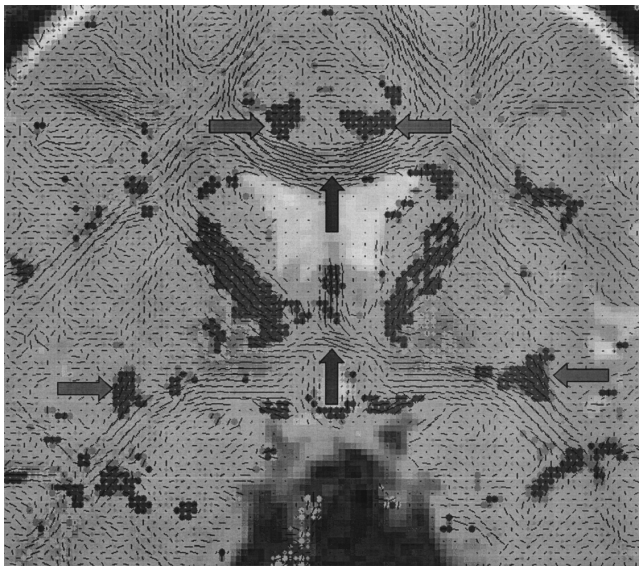

B

FIGURE 55.4. **A:** Sagittal schematic of brain fiber tracks. The vertical line shows the approximate plane of the coronal diffusion tensor image to the right. (Adapted from Gray H, Bannister LH, eds. *Gray's anatomy: the anatomical basis of medicine and surgery,* thirty-eighth ed. London: Churchill Livingstone, 1995.) **B:** In this diffusion tensor imaging (DTI) image, white matter tracts that are within the coronal plane are color-coded blue. Note the corpus callosum *(top blue arrow)* and anterior commissure *(bottom blue arrow)*. White matter tracts perpendicular to the plane are coded red-orange. Note the cingulum bundle *(top arrows),* the white matter tract within the cingulate gyrus, and the uncinate fasiculus *(bottom arrows),* the tract connecting anterior temporal lobe with inferior frontal lobe. (Unpublished image from our laboratory, Shenton et al., 2000; technique and application discussed in Kubicki M, Maier SE, McCarley RW, et al. *Uncinate fasciculus in schizophrenia: a diffusion tensor study.* American Psychiatric Association New Research Abstracts, 2000.) **C:** Parasagittal image showing anterior–posterior course of the cingulate bundle as constructed from DTI. (Unpublished image courtesy of Stephan Maier and Carl-Fredrik Westin, Surgical Planning Laboratory, Brigham and Women's Hospital).

if the adjacent elements have similar linear orientation. This similarity is at the voxel level, and does not, of course, permit tracking of individual fibers; rather, it tracks groups of fibers.

CONCLUSION

A clear current and positive trend is to use as much automation as possible in structural MRI analysis because of the labor involved in traditional ROI analysis. Currently, however, the field is still in a state of flux with respect to the validity of the new techniques, such as VBM and brain warping, because of the absence of detailed comparisons with ROI analysis and formulation of the reasons for differences. Validity evaluation for new technologies is thus a high priority item.

Another clear and positive trend is employ new technologies, and to use multimodal imaging, with diffusion tensor imaging as the prime example within the structural field. Similarly, as discussed in another chapter in this volume by Dr. Berman, ''functional'' imaging is becoming increasingly multimodal and a desideratum is the combination of structural and functional approaches, just as anatomy and physiology are inextricably linked in basic neuroscience studies. The reader will likely notice a certain ''mismatch'' in the brain regions emphasized in the functional imaging chapter (frontal lobe) and in this structural imaging chapter (temporal lobe). It is clear that functional studies have defined more prominent abnormalities in frontal lobe than in temporal lobe, whereas structural studies have tended to show a greater degree of abnormality in temporal lobe. The mismatch may arise, in part, because the frontal lobe receives input from and communicates with virtually all cortical (and many subcortical) areas. Functional neuroimaging ''activation'' in a region primarily represents postsynaptic potentials; these and not action potentials constitute the major metabolic and energetic load and hence the main signals used in functional analysis. It is consequently often very difficult to disambiguate abnormalities in input to frontal lobe from intrinsic abnormalities. Similarly, although temporal lobe gray matter volume changes appear quantitatively larger than those in frontal cortex, no brain region acts on its own and interconnections and abnormalities of interconnections, as well as intrinsic volume changes must be considered in the explanation of the features of schizophrenia. This task of seamlessly integrating information from multiple technologies is both one of the most exciting and also the most challenging for work in the next few years.

APPENDIX A: STRUCTURAL MRI PULSE SEQUENCES

Spin echo pulse sequences use at least two pulses. The first is an initial excitation pulse (tilting the magnetization vector 90 degrees from the steady-state field orientation), followed by one or more refocusing pulses, and directed 180 degrees from the orientation of the steady-state field. These refocusing pulses reintroduce phase coherence (again, the web site *http://ej.rsna.org/ej3/0095-98.fin/index.htm* provides a useful animated illustration of this). The reformation of phase coherence induces another signal known as a ''spin echo,'' which does not have the potential confounds of magnet and tissue inhomogeneity (they remain constant over pulses), and thus this signal provides a better measure of T2. In spin echo pulse sequences the repetition time (TR) is the time between excitation pulses, whereas the echo time (TE) is the time from the excitation pulse to the echo maximum.

Relatively short TR and TE standard single echo sequences produce T1-weighted images. Multiecho sequences produce proton density weighted images at short TE (less than 30 ms) and T2-weighted images at long TE (more than 80 ms) when TR is long enough to allow for nearly compete T1 relaxation (more than 2,000 ms for most tissues). Fast spin echo sequences are a variant of multiecho sequences that maximize efficiency of data collection and shorten acquisition time. They are commonly used to produce T2-weighted images. Inversion recovery pulse sequences are still another variation of the spin echo sequence, in which an additional 180-degree pulse is applied before the excitation pulse, thereby increasing T1 weighting (commonly used for improving contrast between different tissues).

Gradient Echo Pulse Sequences

These sequences do not use 180-degree refocusing pulses. The most commonly used pulse sequence in volumetric work is a spoiled gradient echo sequence, called spoiled GRASS (SPGR) in GE imagers and FLASH in Siemens imagers. This pulse sequence uses a ''spoiling scheme'' to dephase the transverse (x-y plane) magnetization following signal detection, commonly using ''spoiler'' (also called ''crusher'') gradient pulses that have the same duration and magnitude as the first excitation pulse, but the opposite polarity. This has as a consequence that, at the time of the next excitation, only the longitudinal direction (vertical direction in our analogy) has any remaining coherence. If the first pulse has a low excitation angle (small ''tilt'' of the tops in our analogy) this allows shorter repetition times to be used, speeding acquisition.

Signal Intensity of Tissue Elements and T1 and T2 Weighting

SPGR pulses lead to proton density-weighted images, because the small ''tilt'' and short TR diminishes any T1 or T2 effects. In a proton density image produced by the SPGR sequence most commonly used in schizophrenia research, CSF appears dark, gray matter is gray, and white matter

has the most signal (is brightest). Spin-echo sequences can produce proton density, T2- or T1-weighted images. The normal CSF T1 relaxation time is 3,000 ms at 1.5 T, whereas that of fat is 200 to 250 ms; gray matter has a longer T1 relaxation time than white matter and thus shows a brighter signal with sequences allowing longer T1 relaxation times. Because the ability to capture relatively complete T1 relaxation depends on longer TRs, longer TRs thus give brighter CSF and gray matter brighter than white matter. The tissue intensity in T2-weighted images depends on the TE in spin echo sequences. CSF has longer T2 values than other brain tissues and shows up as a bright signal in T2-weighted acquisitions with the long TE values commonly used in schizophrenia volumetric studies. In general, a long TR allows more time for T1 relaxation and produces more signal from tissues with long T1 values, whereas a long TE allows more time for T2 relaxation and produces more signal from tissues with long T2 values.

ACKNOWLEDGMENTS

Supported in part by VA Medical Research Service, Department of Veterans Affairs Center for Clinical and Basic Neuroscience Studies of Schizophrenia, NIMH 40977 and 52807 (RWM). Parts of the introduction are adapted from a previous review: McCarley RW, Wible C, Frumin M, et al. MRI anatomy of schizophrenia. *Biol Psychiatry* 1999;45: 1099–1119.

REFERENCES

1. Kraepelin E (Barclay E, Barclay S, Trans.). *Dementia praecox.* New York: New York: Churchill Livingstone, 1971 (German edition published in 1899).
2. Brown MA, Semelka RC. *MRI: basic principles and applications,* second ed. New York: Wiley-Liss, 1999.
3. Pfefferbaum A, Sullivan EV, Hedehus M, et al. Brain gray and white matter transverse relaxation time in schizophrenia. *Psychiatry Res* 1999;91:93–100.
4. Smith RC, Calderon M, Ravichandran GK, et al. Nuclear magnetic resonance in schizophrenia: A preliminary study. *Psychiatry Res* 1984;12:137–147.
5. Kikinis R, Shenton ME, Jolesz FA, et al. Routine analysis of brain and cerebrospinal fluid spaces with MR imaging. *J Magn Reson Imaging* 1992;2:619–629.
6. Gerig G, Kikinis R, Kubler O. Significant improvement of MR image data quality using anisotropic diffusion filtering. *Technical report BIWI-TR-124.* Zurich: ETH, 1990.
7. Shenton ME, Kikinis R, McCarley RW, et al. Application of automated MRI volumetric measurement techniques to the ventricular system in schizophrenics and normals. *Schizophr Res* 1991;5:103–113.
8. Gur RE, Cowell P, Turetsky BI, et al. A follow-up magnetic resonance imaging study of schizophrenia: relationship of neuroanatomical changes to clinical and neurobehavioral measures. *Arch Gen Psychiatry* 1998;55:145–152.
9. Hunter JE, Schmidt FL. *Methods of metaanalysis.* Newbury Park, CA: Sage, 1990.
10. Petitti DB. *Metaanalysis, decision analysis, and cost-effectiveness analysis.* New York: Oxford University Press, 1994.
11. Rosenthal R. *Judgement studies. Design, analysis and metaanalysis.* Cambridge: Cambridge University Press, 1987.
12. Nelson MD, Saykin AJ, Flashman LA, et al. Hippocampal volume reduction in schizophrenia as assessed by magnetic resonance imaging: a meta-analytic study. *Arch Gen Psychiatry* 1998;55: 433–440.
13. McCarley RW, Wible C, Frumin M, et al. MRI anatomy of schizophrenia. *Biol Psychiatry* 1999;45:1099–1119.
14. Bogerts B. The neuropathology of schizophrenic diseases: historical aspects and present knowledge. *Eur Arch Psychiatry Clin Neurosci* 1999;249(Suppl 4):2–13.
15. Harrison PJ. The neuropathology of schizophrenia. A critical review of the data and their interpretation. *Brain* 1999;122: 593–624.
16. Weinberger DR. Cell biology of the hippocampal formation in schizophrenia. *Biol Psychiatry* 1999;45:395–402.
17. Selemon LD, Rajkowska G, Goldman-Rakic PS. Elevated neuronal density in prefrontal area 46 in brains from schizophrenic patients: application of a three-dimensional stereologic counting method. *J Comp Neurol* 1998;392:402–412.
18. Kikinis R, Shenton ME, Gerig G, et al. Temporal lobe sulcogyral pattern anomalies in schizophrenia: an *in vivo* MR three-dimensional surface rendering study. *Neurosci Lett* 1994;183: 7–12.
19. Iosifescu DV, Shenton ME, Warfield SK, et al. An automated registration algorithm for measuring MRI subcortical brain structures. *Neuroimage* 1997;6:13–25.
20. Schmidt M, Dengler J. Adapting multi-grid methods to the class of elliptic partial differential equation appearing in the estimation of displacement vector fields. In: Cantoni V, Creutzburg R, Levialdi S, et al, eds. *Recent issues in pattern analysis and recognition.* Berlin: Springer, 1989:266—274.
21. Warfield S, Dengler J, Zaers J, et al. Automatic identification of grey matter structures from MRI to improve the segmentation of white matter lesions. *Proceedings of Medical Robotics and Computer Assisted Surgery (MRCAS),* November, 1995;140–47.
22. Grenander U, Miller MI. Representation of knowledge in complex systems. *J R Stat Soc B* 1994;56:3.
23. Collins DL, Peters TM, Dai W, et al. Model based segmentation of individual brain structures from MRI data. *SPIE, Visual Biomed Comput* 1992;1808:10–23.
24. Gee JC, Reivich M, Bajcsy R. Elastically deforming 3D atlas to match anatomical brain images. *J Comput Assist Tomogr* 1993; 17:225–236.
25. Thompson PM, Toga AW. Brain warping. In: Toga AW, ed. *Brain warping.* San Diego: Academic Press, 1999:311–336.
26. Gaser C, Volz H-P, Kiebel S, et al. Detecting structural changes in whole brain based on nonlinear deformations: application to schizophrenia research. *NeuroImage* 1999;10:107–113.
27. Ashburner J, Friston KJ. Voxel-based morphometry: the methods. *NeuroImage* 2000;11:805–821.
28. Wright IC, Ellison ZR, Sharma T, et al. Mapping of grey matter changes in schizophrenia. *Schiz Res* 1999;35:1–14.
29. Casanova MF, Goldberg TE, Suddath RL, et al. Quantitative shape analysis of the temporal and prefrontal lobes of schizophrenic patients: a magnetic resonance image study. *J Neuropsychiatry Clin Neurosci* 1990;2:363–72.
30. Csernansky JG, Joshi S, Wang L, et al. Hippocampal morphometry in schizophrenia by high dimensional brain mapping. *Proc Natl Acad Sci USA* 1998;95:11406–11411.
31. Buchsbaum MS, Tang CY, Peled S, et al. MRI white matter diffusion anisotropy and PET metabolic rate in schizophrenia. *Neuroreport* 1998;9:425–430.
32. Lim KO, Hedehus M, Moseley M, et al. Compromised white

matter tract integrity in schizophrenia inferred from diffusion tensor imaging. *Arch Gen Psychiatry* 1999;56:367–374.
33. Westin CF, Maier SE, Khidhir B, et al. Image processing for diffusion tensor magnetic resonance imaging. In: *Proceedings of Second International Conference on Medical Image Computing and Computer-Assisted Interventions,* Cambridge, UK: 1999:441–452.
34. Kubicki M, Maier SE, McCarley RW, et al. *Uncinate fasciculus in schizophrenia: a diffusion tensor study.* American Psychiatric Association New Research Abstracts, 2000.

Table 55.1 References

Andreasen NC, Ehrhardt JC, Swayze II VW, et al. Magnetic resonance imaging of the brain in schizophrenia: the pathophysiologic significance of structural abnormalities. *Arch Gen Psychiatry* 1990; 47:35–44.

Andreasen NC, Arndt S, Swayze II VW, et al. Thalamic abnormalities in schizophrenia visualized through magnetic resonance image averaging. *Science* 1994a;266:294–298.

Andreasen NC, Flashman L, Flaum M, et al. Regional brain abnormalities in schizophrenia measured with magnetic resonance imaging. *JAMA* 1994b;272:1763–1769.

Barr WB, Ashtari M, Bilder RM, et al. Brain morphometric comparison of first episode schizophrenia and temporal lobe epilepsy. *Br J Psychiatry* 1997;170:515–519.

Barta PE, Pearlson GD, Powers RE, et al. Auditory hallucinations and smaller superior temporal gyral volume in schizophrenia. *Am J Psychiatry* 1990;147:1457–1462.

Barta PE, Pearlson GD, Brill LB, et al. Planum temporale asymmetry reversal in schizophrenia: replication and relationship to gray matter abnormalities. *Am J Psychiatry* 1997a;154:661–667.

Barta PE, Powers RE, Aylward EH, et al. Quantitative MRI volume changes in late onset schizophrenia and Alzheimer's disease compared to normal controls. *Psychiatry Res* 1997b;68:65–75.

Becker T, Elmer K, Mechela B, et al. MRI findings in the medial temporal lobe structures in schizophrenia. *Eur Neuropsychopharmacol* 1990;1:83–186.

Becker T, Elmer K, Schneider F, et al. Confirmation of reduced temporal limbic structure volume on magnetic resonance imaging in male patients with schizophrenia. *Psychiatry Res* 1996;67: 135–143.

Bilder RM, Wu H, Bogerts B, et al. Absence of regional hemispheric volume asymmetries in first-episode schizophrenia. *Am J Psychiatry* 1994;151:1437–1447.

Blackwood DHR, Young AH, McQueen JK, et al. Magnetic resonance imaging in schizophrenia: Altered brain morphology associated with P300 abnormalities and eye tracking dysfunction. *Biol Psychiatry* 1991;30:753–769.

Bogerts B, Ashtari M, Degreef G, et al. Reduced temporal limbic structure volumes on magnetic resonance images in first episode schizophrenia. *Psychiatry Res Neuroimag* 1990;35:1–13.

Bogerts B, Lieberman JA, Ashtari M, et al. Hippocampus-amygdala volumes and psychopathology in chronic schizophrenia. *Biol Psychiatry* 1993;33:236–246.

Bornstein RA, Schwarzkopf SB, Olson SC, et al. Third-ventricle enlargement and neuropsychological deficit in schizophrenia. *Biol Psychiatry* 1992;31:954–961.

Breier A, Buchanan RW, Elkashef A, et al. Brain morphology and schizophrenia: a magnetic resonance imaging study of limbic, prefrontal cortex, and caudate structures. *Arch Gen Psychiatry* 1992; 49:921–926.

Buchanan RW, Breier A, Kirkpatrick B, et al. Structural abnormalities in deficit and nondeficit schizophrenia. *Am J Psychiatry* 1993;150: 59–65.

Buchsbaum MS, Someya T, Teng CY, et al. PET and MRI of the thalamus in never-medicated patients with schizophrenia. *Am J Psychiatry* 1996;153:191–199.

Buchsbaum MS, Yang S, Hazlett E, et al. Ventricular volume and asymmetry in schizotypal personality disorder and schizophrenia assessed with magnetic resonance imaging. *Schizophr Res* 1997; 27:45–53.

Casanova MF, Zito M, Goldberg T, et al. Shape distortion of the corpus callosum of monozygotic twins discordant for schizophrenia. *Schizophr Res* 1990;3:155–156.

Chakos MH, Lieberman JA, Bilder RM, et al. Increase in caudate nuclei volumes of first-episode schizophrenic patients taking antipsychotic drugs. *Am J Psychiatry* 1994;151:1430–1436.

Chakos MH, Lieberman JA, Alvir J, et al. Caudate nuclei volumes in schizophrenic patients treated with typical antipsychotics or clozapine. *Lancet* 1995;345:456–457.

Colombo C, Abbruzzese M, Livian S, et al. Memory functions and temporal limbic morphology in schizophrenia. *Psychiatry Res Neuroimag* 1993;50:45–56.

Colombo C, Bonfanti A, Scarone S. Anatomical characteristics of the corpus callosum and clinical correlates in schizophrenia. *Eur Arch Psychiatry Clin Neurosci* 1994;243:244–248.

Coffman JA, Schwarzkopf SB, Olson SC, et al. Midsagittal cerebral anatomy by magnetic resonance imaging: The importance of slice position and thickness. *Schizophr Res* 1989;2:287–294.

Corey-Bloom J, Jernigan T, Archibald S, et al. Quantitative magnetic resonance imaging of the brain in late-life schizophrenia. *Am J Psychiatry* 1995;152:447–449.

Dauphinais D, DeLisi LE, Crow TJ, et al. Reduction in temporal lobe size in siblings with schizophrenia: a magnetic resonance imaging study. *Psychiatry Res Neuroimag* 1990;35:137–147.

Degreef G, Bogerts B, Ashtari M, et al. Ventricular system morphology in first episode schizophrenia: a volumetric study of ventricular subdivisions on MRI. *Schizophr Res* 1990;3:18.

Degreef G, Ashtari M, Bogerts B, et al. Volumes of ventricular system subdivisions measured from magnetic resonance images in first-episode schizophrenic patients. *Arch Gen Psychiatry* 1992a;49: 531–537.

Degreef G, Bogerts B, Falkai P, et al. Increased prevalence of the cavum septum pellucidum in magnetic resonance scans and postmortem brains of schizophrenic patients. *Psychiatry Res: Neuroimaging* 1992b;45:193–199.

Degreef G, Lantos G, Bogerts B, et al. Abnormalities of the septum pellucidum on MR scans in first-episode schizophrenic patients. *Am J Neuroradiology* 1992c;13:835–840.

DeLisi LE, Hoff AL, Schwartz JE, et al. Brain morphology in first-episode schizophrenic-like psychotic patients: a quantitative magnetic resonance imaging study. *Biol Psychiatry* 1991;29:159–175.

DeLisi LE, Strizke P, Riordan H, et al. The timing of brain morphological changes in schizophrenia and their relationship to clinical outcome. *Biol Psychiatry* 1992;31:241–254.

DeLisi LE, Hoff AL, Kushner M, et al. Increased prevalence of cavum septum pellucidum in schizophrenia. *Psychiatry Res: Neuroimag* 1993;50:193–199.

DeLisi LE, Hoff AL, Neale C, et al. Asymmetries in the superior temporal lobe in male and female first-episode schizophrenic patients: measures of the planum temporale and superior temporal gyrus by MRI. *Schizophr Res* 1994;12:19–28.

DeLisi LE, Sakuma M, Tew W, et al. Schizophrenia as a chronic active brain process: a study of progressive brain structural change subsequent to the onset of schizophrenia. *Psychiatry Res* 1997;74: 129–140.

DeQuardo JR, Bookstein FL, Green WD, et al. Spatial relationships of neuroanatomic landmarks in schizophrenia. *Psychiatry Res* 1996; 67:81–95.

Di Michele V, Rossi A, Stratta P, et al. Neuropsychological and clini-

cal correlates of temporal lobe anatomy in schizophrenia. *Acta Psychiatr Scand* 1992;85:484–488.

Egan MF, Duncan CC, Suddath RL, et al. Event-related potential abnormalities correlate with structural brain alterations and clinical features in patients with chronic schizophrenia. *Schizophr Res* 1994;11:259–271.

Elkashef AM, Buchanan RW, Gellad F, et al. Basal ganglia pathology in schizophrenia and tardive dyskinesia: an MRI quantitative study. *Am J Psychiatry* 1994;151:752–755.

Flaum M, Swayze II VW, O'Leary DS, et al. Effects of diagnosis and gender on brain morphology in schizophrenia. *Am J Psychiatry* 1995b;152:704–714.

Fukuzako T, Fukuzako H, Kodama S, et al. Cavum septum pellucidum in schizophrenia: a magnetic resonance imaging study. *Psychiatry Clin Neurol* 1996a;:125–128.

Fukuzako H, Fukuzako T, Hashiguchi T, et al. Reduction in hippocampal formation volume is caused mainly by its shortening in chronic schizophrenia: assessment by MRI. *Biol Psychiatry* 1996b; 39:938–945.

Gunther W, Petsch R, Steinberg R, et al. Brain dysfunction during motor activation and corpus callosum alterations in schizophrenia measured by cerebral blood flow and magnetic resonance imaging. *Biol Psychiatry* 1991;29:535–555.

Gur RE, Mozley PD, Shtasel DL, et al. Clinical subtypes of schizophrenia: differences in brain and CSF volume. *Am J Psychiatry* 1994;151:343–350.

Gur RE, Cowell P, Turetsky BI, et al. A follow-up magnetic resonance imaging study of schizophrenia: relationship of neuroanatomical changes to clinical and neurobehavioral measures. *Arch Gen Psychiatry* 1998;55:145–152.

Hajek M, Huonker R, Boehle C, et al. Abnormalities of auditory evoked magnetic fields and structural changes in the left hemisphere of male schizophrenics—a magnetoencephalographic-magnetic resonance imaging study. *Biol Psychiatry* 1997;42:609–616.

Harvey J, Ron MA, Boulay GD, et al. Reduction of cortical volume in schizophrenia on magnetic resonance imaging. *Psychol Med* 1993;23:591–604.

Hauser PI, Dauphinais D, Berrettini W, et al. Corpus callosum dimensions measured by magnetic resonance imaging in bipolar affective disorder and schizophrenia. *Biol Psychiatry* 1989;26: 659–668.

Hirayasu Y, Shenton ME, Salisbury DF, et al. Lower left temporal lobe MRI volumes in patients with first-episode schizophrenia compared with psychotic patients with first-episode affective disorder and normal subjects. *Am J Psychiatry* 1998a;155:1384–1391.

Hoff AL, Riordan H, O'Donnell D, et al. Anomalous lateral sulcus and cognitive function in first-episode schizophrenia. *Schizophr Bull* 1992;18:257–272.

Hoff AL, Neal C, Kushner M, et al. Gender differences in corpus callosum size in first-episode schizophrenics. *Biol Psychiatry* 1994; 35:913–919.

Hokama H, Shenton ME, Nestor PG, et al. Caudate, putamen, and globus pallidus volume in schizophrenia: a quantitative MRI study. *Psychiatry Res Neuroimag* 1995;61:209–229.

Jernigan TL, Zisook S, Heaton RK, et al. Magnetic resonance imaging abnormalities in lenticular nuclei and cerebral cortex in schizophrenia. *Arch Gen Psychiatry* 1991;48:881–890.

Johnstone EC, Owens DGC, Crow TJ, et al. Temporal lobe structure as determined by nuclear magnetic resonance in schizophrenia and bipolar affective disorder. *J Neurol Neurosurg Psychiatry* 1989;52: 736–741.

Jurjus GJ, Nasrallah HA, Olson SC, et al. Cavum septum pellucidum in schizophrenia, affective disorder, and healthy controls: a magnetic resonance imaging study. *Psychol Med* 1993;23:319–322.

Kawasaki Y, Maeda Y, Urata K, et al. A quantitative magnetic resonance imaging study of patients with schizophrenia. *Eur Arch Psychol Clin Neurosci* 1993;242:268–272.

Kelsoe JR, Cadet JL, Pickar D, et al. Quantitative neuroanatomy in schizophrenia: a controlled magnetic resonance imaging study. *Arch Gen Psychiatry* 1988;45:533–541.

Keshavan MS, Bagwell WW, Haas GL, et al. Does caudate volume increase during follow up in first-episode psychosis? *Schizophr Res* 1995;15:87.

Kikinis R, Shenton ME, Gerig G, et al. Temporal lobe sulco-gyral pattern anomalies in schizophrenia: an in vivo MR three-dimensional surface rendering study. *Neuroscience Lett* 1994;182:7–12.

Kleinschmidt P, Falkai P, Huang Y, et al. In vivo morphometry of planum temporale asymmetry in first-episode schizophrenia. *Schizophr Res* 1994;12:9–18.

Kulynych JJ, Vladar K, Fantie BD, et al. Normal asymmetry of the planum temporale in patients with schizophrenia: three-dimensional cortical morphometry with MRI. *Br J Psychiatry* 1995;166: 742–749.

Kulynych JJ, Vladar K, Jones DW, et al. Superior temporal gyrus volume in schizophrenia: a study using MRI morphometry assisted by surface rendering. *Am J Psychiatry* 1996;153:50–56.

Kwon JS, Shenton ME, Hirayasu Y, et al. MRI study of cavum septi pellucidi in schizophrenia, affective disorder, and schizotypal personality disorder. *Am J Psychiatry* 1998;155:509–515.

Kwon JS, McCarley RW, Hirayasu Y, et al. Left planum temporale volume reduction in schizophrenia. *Arch Gen Psychiatry* 1999;56: 142–148.

Lauriello J, Hoff A, Wieneke MH, et al. Similar extent of brain dysmorphology in severely ill women and men with schizophrenia. *Am J Psychiatry* 1997;154:819–825.

Lewine RR, Gulleu LR, Risch SC, et al. Sexual dimorphism, brain morphology, and schizophrenia. *Schizophr Bul* 1990;16:195–203.

Lim KO, Tew W, Kushner M, et al. Cortical gray matter volume deficit in patients with first-episode schizophrenia. *Am J Psychiatry* 1996;153:1548–1553.

Marsh L, Suddath RL, Higgins N, et al. Medial temporal lobe structures in schizophrenia: relationship of size to duration of illness. *Schizophr Res* 1994;11:225–238.

Marsh L, Harris D, Lim KO, et al. Structural magnetic resonance imaging abnormalities in men with severe chronic schizophrenia and an early age at clinical onset. *Arch Gen Psychiatry* 1997;54: 1104–1112.

Menon RR, Barta PE, Aylward EH, et al. Posterior superior temporal gyrus in schizophrenia: grey matter changes and clinical correlates *Schizophr Res* 1995;16:127–135.

Mion CC, Andreasen NC, Arndt S, et al. MRI abnormalities in tardive dyskinesia. *Psychiatry Res Neuroimag* 1991;40:157–166.

Nasrallah HA, Schwarzkopf SB, et al. Gender differences in schizophrenia on MRI brain scans. *Schizophr Bull* 1990;16:205–210.

Nopoulos P, Torres I, Flaum M, et al. Brain morphology in first-episode schizophrenia. *Am J Psychiatry* 1995;152:1721–1723.

Nopoulos P, Swayze V, Andreasen NC. Pattern of brain morphology in patients with schizophrenia and large cavum septi pellucidi. *J Neuropsychiatry Clin Neurosci* 1996;8:147–152.

Nopoulos P, Swayze V, Flaum M, et al. Cavum septi pellucidi in normals and patients with schizophrenia as detected by magnetic resonance imaging. *Biol Psychiatry* 1997;41:1102–1108.

Ohnuma T, Kimura N, Takahashi T, et al. A magnetic resonance imaging study in first episode disorganized-type patients with schizophrenia. *Psychiatry Clin Neurosci* 1997;51:9–15.

Petty RG, Barta PE, Pearlson GD, et al. Reversal of asymmetry of the planum temporale in schizophrenia. *Am J Psychiatry* 1995; 152:715–721.

Portas CM, Goldstein JM, Shenton ME, et al. Volumetric evaluation of the thalamus in schizophrenic male patients using magnetic resonance imaging. *Biol Psychiatry* 1998;43:649–659.

Raine A, Harrison GN, Reynolds GP, et al. Structural and functional characteristics of the corpus callosum in schizophrenics. *Arch Gen Psychiatry* 1990;47:1060–1064.

Raine A, Lencz T, Reynolds GP, et al. An evaluation of structural and functional prefrontal deficits in schizophrenia: MRI and neuropsychological measures. *Psychiatry Res Neuroimag* 1992;45: 123–137.

Reite M, Sheeder J, Teale P, et al. Magnetic source imaging evidence of sex differences in cerebral lateralization in schizophrenia. *Arch Gen Psychiatry* 1997;54:433–440.

Rossi A, Stratta P, Gallucci M, et al. Standardized magnetic resonance image intensity study in schizophrenia. *Psychiatry Res* 1988;25: 223–231.

Rossi A, Stratta P, Galluci M, et al. Quantification of corpus callosum and ventricles in schizophrenics with nuclear magnetic resonance imaging: a pilot study. *Am J Psychiatry* 1989a;46:99–101.

Rossi A, Stratta P, D'Albenzio L, et al. Reduced temporal lobe area in schizophrenia by magnetic resonance imaging: preliminary evidence. *Psychiatry Res* 1989b;29:261–263.

Rossi A, Stratta P, D'Albenzio L, et al. Reduced temporal lobe areas in schizophrenia: preliminary evidences from a controlled multiplanar magnetic resonance imaging study. *Biol Psychiatry* 1990b; 27:61–68.

Rossi A, Stratta A, Michele VD, et al. Temporal lobe structure by magnetic resonance in bipolar affective disorders and schizophrenia. *J Affective Dis* 1991;21:19–22.

Rossi A, Stratta P, Mattei P, et al. Planum temporale in schizophrenia: a magnetic resonance study. *Schizophr Res* 1992;7:19–22.

Rossi A, Stratta P, Mancini F, et al. Cerebellar vermal size in schizophrenia: a male effect. *Biol Psychiatry* 1993;33:354–357.

Rossi A, Serio A, Stratta P, et al. Planum temporale asymmetry and thought disorder in schizophrenia. *Schizophr Res* 1994a;12:1–7.

Rossi A, Stratta P, Mancini F, et al. Magnetic resonance imaging findings of amygdala-anterior hippocampus shrinkage in male patients with schizophrenia. *Psychiatry Res* 1994b;52:43–53.

Schlaepfer TE, Harris GJ, Tien AY, et al. Decreased regional cortical gray matter volume in schizophrenia. *Am J Psychiatry* 1994;151: 842–848.

Schwartz JM, Aylward E, Barta PE, et al. Sylvian fissure size in schizophrenia measured with the magnetic resonance imaging rating protocol of the consortium to establish a registry for Alzheimer's disease. *Am J Psychiatry* 1992;149:1195–1198.

Schwarzkopf SB, Olson SC, Coffman JA, et al. Third and lateral ventricular volumes in schizophrenia: support for progressive enlargement of both structures. *Psychopharm Bull* 1990;26:385–391.

Scott TF, Price TP, George MS, et al. Midline cerebral malformations and schizophrenia. *J Neuropsychiatry Clin Neurosci* 1993;5: 287–293.

Shenton ME, Kikinis R, McCarley RW, et al. Application of automated MRI volumetric measurement techniques to the ventricular system in schizophrenics and normal controls. *Schizophr Res* 1991; 5:103–113.

Shenton ME, Kikinis R, Jolesz FA, et al. Abnormalities of the left temporal lobe and thought disorder in schizophrenia: a quantitative magnetic resonance imaging study. *N Engl J Med* 1992;327: 604–612.

Shioiri T, Oshitani Y, Kato T, et al. Prevalence of cavum septum pellucidum detected by MRI in patients with bipolar disorder, major depression and schizophrenia. *Psychol Med* 1996;26: 431–434.

Stratta P, Rossi A, Gallucci M, et al. Hemispheric asymmetries and schizophrenia: a preliminary magnetic resonance imaging study. *Biol Psychiatry* 1989;25:275–284.

Suddath RL, Casanova MF, Goldberg TE, et al. Temporal lobe pathology in schizophrenia: a quantitative magnetic resonance imaging study. *Am J Psychiatry* 1989;146:464–472.

Suddath RL, Christison GW, Torrey EF, et al. Anatomical abnormalities in the brains of monozygotic twins discordant for schizophrenia. *N Engl J Med* 1990;332:789–794.

Sullivan EV, Mathalon DH, Lim KO, et al. Patterns of regional cortical dysmorphology distinguishing schizophrenia and chronic alcoholism. *Biol Psychiatry* 1998;43:118–131.

Swayze II VW, Andreasen NC, Alliger RJ, et al. Subcortical and temporal structures in affective disorder and schizophrenia: a magnetic resonance imaging study. *Biol Psychiatry* 1992;31:221–240.

Tune L, Barta P, Wong D, et al. Striatal dopamine D2 receptor quantification and superior temporal gyrus: volume determination in 14 chronic schizophrenic subjects. *Psychiatry Res* 1996;67: 155–158.

Uematsu M, Kaiya H. The morphology of the corpus callosum in schizophrenia: an MRI study. *Schizophr Res* 1988;1:391–398.

Uematsu M, Kaiya H. Midsagittal cortical pathomorphology of schizophrenia: a magnetic resonance imaging study. *Psychiatry Res* 1989;30:11–20.

Vita A, Dieci M, Giobbio GM, et al. Language and thought disorder in schizophrenia: brain morphological correlates. *Schizophr Res* 1995;15:243–251.

Wible CG, Shenton ME, Hokama H, et al. Prefrontal cortex and schizophrenia: a quantitative magnetic resonance imaging study. *Arch Gen Psychiatry* 1995;52:279–288.

Woodruff PW, Pearlson GD, Geer MJ, et al. A computerized magnetic resonance imaging study of corpus callosum morphology in schizophrenia. *Psychol Med* 1993;23:45–56.

Woodruff PW, Wright IC, Shuriquie N, et al. Structural brain abnormalities in male schizophrenics reflect fronto-temporal dissociation. *Psychol Med* 1997a;27:1257–1266.

Woodruff PW, Philips ML, Rushe T, et al. Corpus callosum size and inter-hemispheric function in schizophrenia. *Schizophr Res* 1997b; 23:189–196.

Woods BT, Yurgelun-Todd D, Goldstein JM, et al. MRI Brain abnormalities in chronic schizophrenia: one process or more? *Biol Psychiatry* 1996;40:585–596.

Zipursky RB, Lim DO, Sullivan EV, et al. Widespread cerebral gray matter volume deficits in schizophrenia. *Arch Gen Psychiatry* 1992; 49:195–205.

Zipursky RB, Marsh L, Lim KO, et al. Volumetric MRI assessment of temporal lobe structures in schizophrenia. *Biol Psychiatry* 1994; 35:501–516.

Zipursky RB, Seeman MV, Bury A, et al. Deficits in gray matter volume represent in schizophrenia but not bipolar disorder. *Schizophr Res* 1997;26:85–92.